Exposure to China dust exacerbates testicular toxicity induced by cyclophosphamide in mice

Woong-Il Kim[1] · Je-Oh Lim[1] · So-Won Pak[1] · Se-Jin Lee[1] · In-Sik Shin[1] · Changjong Moon[1] · Jeong-Doo Heo[2] · Jong-Choon Kim[1]

Abstract

This study investigated the potential effects of China dust (CD) exposure on cyclophosphamide (CP)-induced testicular toxicity in mice, focusing on spermatogenesis and oxidative damage. CP treatment reduced testicular and epididymal weight and sperm motility and enhanced sperm abnormality. Histopathological examination presented various morphological alterations in the testis, including increased exfoliation of spermatogenic cells, degeneration of early spermatogenic cells, vacuolation of Sertoli cells, a decreased number of spermatogonia/spermatocytes/spermatids, along with a high number of apoptotic cells. In addition, the testis exhibited reduced glutathione (GSH) levels and glutathione reductase (GR) activity and enhanced malondialdehyde (MDA) concentration. Meanwhile, CD exposure exacerbated testicular histopathological alterations induced by CP. CD exposure also aggravated oxidative damage by increasing the lipid peroxidative product MDA and decreasing GSH levels and antioxidant enzyme activities in the testis. These results suggest that CD exposure exacerbates CP-induced testicular toxicity in mice, which might be attributed to the induction of lipid peroxidation and reduced antioxidant activity.

Keywords Cyclophosphamide · China dust · Testicular toxicity · Oxidative damage · Apoptotic cells

Introduction

Cyclophosphamide (CP) is one of the oldest cancer chemotherapy drugs introduced in 1958 [1]. It has been widely used as an anticancer agent to treat cancers such as leukemia, lymphoma, ovarian carcinoma, and breast carcinoma [2]. However, similar to other anticancer agents with side effects, the application of CP has been limited owing to various side effects, including reproductive toxicity [3]. Based on the known pharmacological activity, CP inhibits rapidly dividing cells, which are abundantly present in the reproductive system, thus increasing their susceptibility to CP [3]. Moreover, gonadotropin secretion disorders, low blood testosterone levels, histological changes in the testes and epididymides, oligospermia, and azoospermia have been observed in male subjects treated with CP, resulting in reproductive dysfunctions [4, 5]. Although the precise mechanism underlying CP-mediated testicular dysfunction remains unknown, some studies have suggested that acrolein, a CP metabolite, induces oxidative stress and causes testicular toxicity [6, 7]. Acrolein inhibits the tissue antioxidant defense system by producing reactive oxygen species (ROS) and reacts with amino acids to negatively impact enzymes [8, 9]. High ROS levels induce oxidative DNA damage and sperm dysfunction. Furthermore, spermatozoa are vulnerable to peroxidative damage, given the high content of polyunsaturated fatty acids in the plasma membrane and low concentration of scavenging enzymes in the cytoplasm [10]. Therefore, it is speculated that CP-induced testicular toxicity may be exacerbated by other substances known to induce oxidative stress.

China dust (CD), a type of fine particulate matter (PM), is a meteorological phenomenon originating from the deserts of Mongolia and northern China. In recent years, the potential health effects of CD have raised public concerns

✉ Jong-Choon Kim
toxkim@jnu.ac.kr

1 College of Veterinary Medicine, Chonnam National University, 77 Yongbong-ro, Buk-gu, 61186 Gwangju, Republic of Korea

2 Bioenvironmental Science & Technology Division, Korea Institute of Toxicology, 52834 Jinju, Republic of Korea

in Northeast Asia, including Korea and Japan [11, 12]. Dust can travel long distances and absorb various components such as inorganic ions, and more broadly, organic ions, carbon, metal, and polycyclic aromatic hydrocarbons from anthropogenic sources in industrial areas [13, 14].

PM exposure can induce inhibition of cell proliferation, cell cycle changes, apoptosis, and DNA damage, but the precise underlying mechanism that induces these effects remains elusive [15, 16]. However, it is speculated that the biological response could be attributed to the oxidative potential of particles coming into direct contact with biological fluids or cellular molecules to form ROS or oxidize substrates [16–18]. Therefore, as exposure to PM induces various toxicities through oxidative stress, it is highly likely that the oxidative stress-mediated toxic potential of PM is enhanced following simultaneous exposure to CP. The purpose of this study was to determine whether CD, a type of fine PM, exacerbates CP-induced testicular toxicity.

Materials and methods

Experimental animals and environmental conditions

A total of 30 male BALB/c mice (9-weeks old) were obtained from a specific pathogen-free colony at SAM-TAKO Co. (Osan, Korea) and used after 1 week of quarantine and acclimatization. Three mice per polycarbonate cage were maintained at a temperature of $22 \pm 2°C$ and $55 \pm 5\%$ relative humidity, with a 12 h light/dark cycle, 13–18 air changes/h, with free access to standard rodent diet and water. The animals were maintained in accordance with the Guide for the Care and Use of Laboratory Animals [19] as well as following the 3R principles [20]. The experimental protocol was performed in accordance with the protocol of the CNU Institutional Animal care and Use Committee (CNU IACUC-YB-2020-109).

Test substances and treatment

CP was obtained from Sigma-Aldrich (St. Louis, MO, USA). CD was obtained from Powder Technology Inc. (Arden Hills, MN, USA) and consisted of 50% JIS Z8901 Class 8 (SiO_2, Al_2O_3, Fe_2O_3, MgO, CaO, TiO_2) and 50% natural SiO_2. Both CP and CD were dissolved in phosphate-buffered saline (PBS) and prepared prior to administration. CP (200 mg/kg) and CD (20 and 40 mg/kg) doses were computed based on the body weight of each mouse immediately prior to administration. CP was injected intraperitoneally on day 1. CD was intranasally administered under slight anesthesia using isoflurane (Isotroy®, Troikaa Pharmaceuticals Ltd., Gujarat, India), three times on days 1, 3, and 5.

Physicochemical characterization of CD

The morphology and primary size of CD were measured using transmission electron microscope (TEM; JEM-2100 F, JEOL, Tokyo, Japan) and scanning electron microscopy (SEM; Zeiss Gemini500, Carl Zeiss Meditec AG, Jena, Germany) at accelerating voltages of 150 kV and 15 kV, respectively. Samples for TEM analysis were prepared by dropping a solution of suspended CD on carbon-coated nickel grids. Samples for SEM analysis were scattered on a double-sided carbon adhesive tape onto an aluminum SEM stub and then dusted to release loose particles. The purity of CD was measured by energy dispersive X-ray spectroscopy (Zeiss Gemini500 SEM equipped with X-Max^N 150 mm^2 silicon drift detector; Oxford Instrument, Abingdon, UK). The hydrodynamic size of CD was determined by ELS-8000 (Otsuka Electronic, Tokyo, Japan).

Experimental group and dose selection

Thirty mature male mice were randomized into five groups (n = 6) as follows: (1) normal control group (NC), administered PBS only; (2) CP group received an intraperitoneal injection of CP at 200 mg/kg on day 1 and an intranasal instillation of PBS on days 1, 3, and 5; (3) CD40 group received an intraperitoneal injection of PBS on day 1 and an intranasal instillation of CD at 40 mg/kg on days 1,3, and 5; (4) CP+CD20 group received an intraperitoneal injection of CP at 200 mg/kg on day 1 and an intranasal instillation of CD at 20 mg/kg on days 1,3, and 5; (5) CP+CD40 group received an intraperitoneal injection of CP at 200 mg/kg on day 1 and an intranasal instillation of CD at 40 mg/kg on days 1,3, and 5. The CP dose was determined based on previous studies that established testicular toxicity in mice [21, 22]. The CD doses were selected based on preliminary experimental results and our previous studies related to SiO_2, the major CD component [23, 24]. A preliminary experiment was performed at CD concentrations of 20, 40, and 80 mg/kg with the same protocol as this experiment, and inflammatory cytokines in the bronchoalveolar lavage fluid and pathological lesions of the lung tissue were significantly increased in the ≥40 mg/kg groups compared to the NC group.

Clinical observations and necropsy

Mice were observed daily for any clinical signs of toxicity during the experimental period. Body weights were measured at the start of the experiment and days 3, 5, and 7. On

day 7, all mice were anesthetized with alfaxalone (Jurox, Australia) and euthanized by aortic exsanguination. Absolute weights for the testes and epididymides were measured and were converted to relative organ weights based on the organ-to-body weight ratio.

Sperm examination

Sperm analysis was performed as detailed previously [25]. For sperm motility analysis, seminal fluid was extracted by cutting the tail of the right epididymis with scissors and then placed in a Petri dish containing Hanks' balanced salt solution (Sigma-Aldrich) with 5 mg/mL bovine serum albumin at a pH 7.2, followed by incubation at 37 °C for 5 min. Sperm motility was observed directly using a microscope in a stage warmer. Spermatozoa were considered motile if they showed any movement. For examining sperm morphology, the sperm suspension was smeared on a glass slide and stained with 1% Eosin Y. In total, 100 sperm per animal were microscopically evaluated for head and tail abnormalities and then grouped into the following categories: normal, amorphous head, small head, two heads/tails, excessive hook, straight hook, folded tail, short tail, and no tail.

Histopathologic examination

After harvesting, the left testis was fixed in Bouin's solution for one week, dehydrated, embedded in paraffin, and sectioned at 4-μm thickness. Next, the sections were stained with hematoxylin-eosin (Sigma-Aldrich) and examined under a microscope as previously described [26, 27].

Quantitative morphometry of spermatogenic cells

The mouse spermatogenic cycle can be divided into 12 stages, and each stage is distinguished by unique and specific characteristics of the spermatogenic cells [28]. Using a microscope, we counted the numbers of spermatogonia, preleptotene spermatocytes, zygotene spermatocytes, pachytene spermatocytes, round spermatids, elongated spermatids, and Sertoli cells in seminiferous tubules at stages II, V, VII, and XII of the spermatogenic cycle. In addition, five seminiferous tubules per mouse exhibiting a round shape were randomly selected for each stage of the spermatogenic cycle.

Oxidative stress analysis

Each frozen right testis was placed in MT Cell Lysis Reagent (1 mL), phosphatase inhibitor cocktail (1 μL), and protease inhibitor cocktail (1/10 tablet) and then homogenized using grinding bead P2 and Gene ready Ultracool (Daejeon,

Korea). Next, the homogenates were centrifuged at 14,000 × g for 12 min at 4 °C to remove any cell debris; the supernatant was assayed using suitable kits to estimate glutathione (GSH; Dogenbio, Seoul, Korea), glutathione reductase (GR), catalase (CAT), and malondialdehyde (MDA; Cayman, Ann Arbor, MI, USA).

Terminal deoxynucleotidyl transferase (TdT) dUTP nick-end labeling (TUNEL) assay

TUNEL assay was performed according to the ApopTag® peroxidase In Situ Apoptosis Detection Kit (Millipore, Billerica, MA, USA). Apoptotic cells exhibited brown staining. The number of TUNEL-positive cells was counted in five different fields in each section under × 200 magnification.

Statistical analysis

Data values are expressed as means ± standard deviation. Statistical comparison was performed by one-way analysis of variance, followed by Dunnett's test for multiple comparisons. Results were considered statistically significant at $p < 0.05$ or 0.01. Statistical analyses were performed using GraphPad InStat v.3.0 (GraphPad Software, Inc., San Diego, CA, USA).

Results

Physicochemical characterization of CD

The morphology of CD was generally spherical shape confirmed by SEM and TEM analyses (Fig. 1A, B). CD consisted of O 51.46%, Si 35.38%, Al 6.27%, Fe 5.64%, Mg 0.49%, Ti 0.46%, Ca 0.3% as determined using energy-dispersive X-ray spectroscopy on the same images of SEM (Fig. 1C). The actual size of CD determined by SEM was 43.4 ± 17.7 nm (300 counts) and the hydrodynamic size of CD was 504.2 ± 135.5 nm in water.

Effects of CD on clinical signs and mortality

During the study period, no treatment-related adverse effects were observed in the NC and CD40 groups in terms of clinical signs and mortality (data not shown). However, CP treatment increased the incidence of treatment-related clinical findings, including decreased locomotor activity, soft stool, and anorexia. In addition, the incidence and severity of clinical findings were slightly higher in the CP + CD groups than in the CP group, with no significant difference observed between groups.
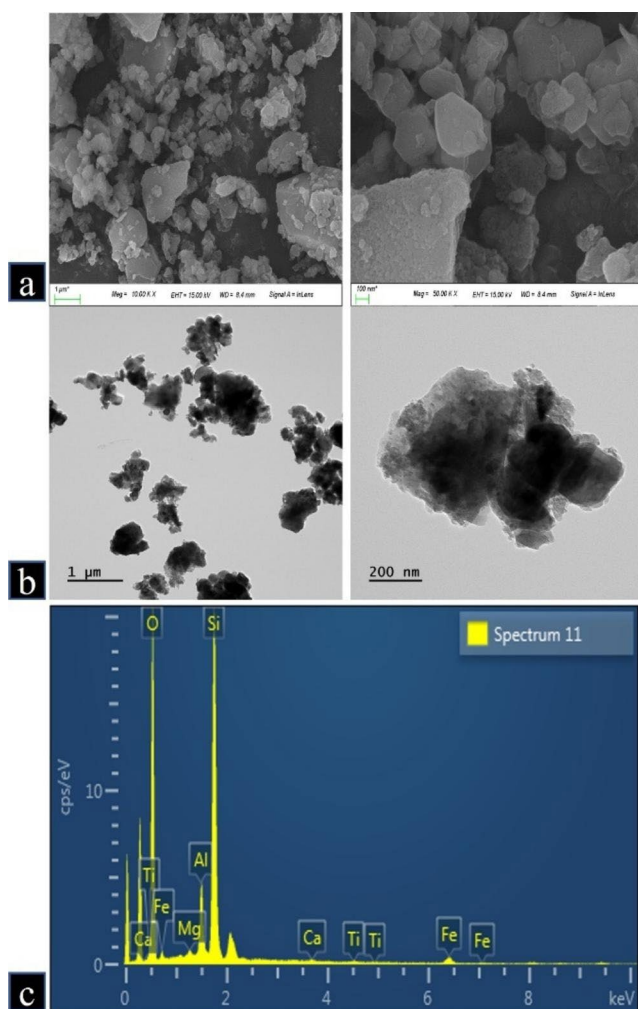
Fig. 1 Morphology and purity of China dust (CD). (**a, b**) Morphology of CD was measured by scanning electron microscopy and transmission electron microscopy. (**c**) Purity of CD was measured by energy-dispersive X-ray spectroscopy (O: 51.46%, Si: 35.38%, Al: 6.27%, Fe: 5.64%, Mg: 0.49%, Ti: 0.46%, Ca: 0.3%)

Effects of CD on body weight and reproductive organ weights

As shown in Table 1, the body weight and absolute weights of testes and epididymides were remarkably declined in the CP group compared to the NC group. In addition, the absolute weights of the testes and epididymides in the CP+CD groups tended to decrease when compared with those in the CP group, and the terminal body weight was significantly lower in the CP+CD40 group than that in the CP group.

Effects of CD on sperm features

Table 2 summarizes the results of the epididymal sperm examination. Compared with the NC group, epididymal sperm motility was significantly reduced in the CP group.

The epididymal sperm motility showed a tendency to decrease in the CP+CD groups when compared with that in the CP group; however, no significant differences were detected between CP and CP+CD groups. Abnormalities in sperm morphology were significantly increased in the CP and CP+CD groups when compared with that in the NC group, given the increased incidence of folded tail; however, no significant differences were noted between the CP and CP+CD groups.

Effects of CD on histopathology findings

The results of the testicular histopathologic examination are presented in Table 3; Fig. 2. The NC and CD40 groups showed normal testicular architecture. However, testicular tissue in the CP group exhibited slight-to-moderate histopathological alterations, such as spermatogenic cell exfoliation, degeneration of spermatogonium/spermatocyte, and reduced number of spermatogonia/spermatocytes, as well as vacuolation of Sertoli cells. The incidence and severity of histopathological alterations were substantially higher in the CP+CD groups than in the CP group.

In the quantitative morphometric analysis of spermatogenic epithelia (Table 4), the numbers of spermatogonia and pachytene spermatocytes at stage II spermatogonia, pachytene spermatocytes, and round spermatids at stage V; preleptotene spermatocytes and pachytene spermatocytes at stage VII; and zygotene spermatocytes and pachytene spermatocytes at stage XII were significantly lower in the CP group than in the NC group. Moreover, the numbers of spermatogonia and pachytene spermatocytes at stage II, preleptotene spermatocytes at stage VII, and zygotene spermatocytes at stage XII in the CP+CD20 and CP+CD40 groups, as well as the number of pachytene spermatocytes at stage V in the CP+CD40 group, were significantly lower than in the CP group.

Effects of CD on antioxidant balance

Table 5 presents GSH and MDA concentrations and antioxidant enzyme activities in testicular tissues. Compared with the NC group, the CP group exhibited significantly reduced GSH levels and GR activity. CAT activity in the CP group was also decreased when compared with the NC group, but no significant difference was detected between groups. Compared with the NC group, the CP group presented a significantly elevated MDA concentration. Compared with the CP group, the decreased GSH level and GR and CAT activities, as well as the increased MDA concentration, were further exacerbated in CP+CD groups. The GSH content and GR and CAT activities were significantly reduced in the CP+CD40 group when compared with those in the CP

Table 1 Reproductive organ weights of the male mice treated with cyclophosphamide (CP) and/or China dust (CD)

Parameters	Group				
	NC	CP	CD40	CP + CD20	CP + CD40
No. of mice examined	6	6	6	6	6
Body weight at term	24.20 ± 1.170[a]	20.37 ± 0.563[**]	24.55 ± 1.408	19.47 ± 1.434[**]	18.53 ± 1.061[**,†]
Testis: left (g)	0.096 ± 0.0061	0.082 ± 0.0035[**]	0.095 ± 0.0073	0.081 ± 0.0070[**]	0.080 ± 0.0044[**]
per body weight (%)	0.396 ± 0.0192	0.402 ± 0.0199	0.386 ± 0.0228	0.415 ± 0.0331	0.431 ± 0.0251
Testis: right (g)	0.094 ± 0.0053	0.083 ± 0.0065[*]	0.096 ± 0.0080	0.081 ± 0.0059[**]	0.079 ± 0.0064[**]
per body weight (%)	0.391 ± 0.0259	0.406 ± 0.0246	0.392 ± 0.0209	0.415 ± 0.0175	0.427 ± 0.0291
Epididymis: left (g)	0.032 ± 0.0011	0.025 ± 0.0020[**]	0.031 ± 0.0026	0.024 ± 0.0021[**]	0.024 ± 0.0012[**]
per body weight (%)	0.131 ± 0.0095	0.121 ± 0.0113	0.126 ± 0.0066	0.124 ± 0.0077	0.129 ± 0.0046
Epididymis: right (g)	0.030 ± 0.0016	0.025 ± 0.0019[**]	0.030 ± 0.0019	0.022 ± 0.0029[**]	0.023 ± 0.0016[**]
per body weight (%)	0.126 ± 0.0079	0.122 ± 0.0081	0.124 ± 0.0057	0.115 ± 0.0130	0.123 ± 0.0080

[a] Values are presented as means ± SD. [*] $p < 0.05$ vs. NC group; [**] $p < 0.01$ vs. NC group; [†] $p < 0.05$ vs. CP group, respectively

Table 2 Sperm analysis of male mice treated with cyclophosphamide (CP) and/or China dust (CD)

Parameters	Group				
	NC	CP	CD40	CP + CD20	CP + CD40
No. of mice examined	6	6	6	6	6
Sperm motility (%)	71.8 ± 7.57[a]	49.8 ± 7.81[**]	71.3 ± 3.56	44.5 ± 7.92[**]	41.3 ± 10.42[**]
Sperm abnormality (%)	19.8 ± 5.34	31.7 ± 3.27[**]	25.2 ± 5.04	31.3 ± 4.23[**]	33.2 ± 3.97[**]
Small head	0	0.3 ± 0.52	0.2 ± 0.41	0.5 ± 0.55	0.3 ± 0.52
Amorphous head	10.5 ± 4.04	13.5 ± 1.87	12.8 ± 5.12	12.7 ± 3.33	15.0 ± 6.13
Two heads/tail	0.5 ± 0.84	1.5 ± 1.05	0.8 ± 0.75	0.5 ± 0.84	0.5 ± 0.55
Excessive hook	0.2 ± 0.41	0.8 ± 0.98	0	0.8 ± 1.60	0.8 ± 1.33
Straight hook	0.2 ± 0.41	0.3 ± 0.52	0	0.2 ± 0.41	0.2 ± 0.41
Folded tail	7.3 ± 3.39	13.3 ± 1.21[**]	9.3 ± 3.72	13.0 ± 3.79[*]	12.5 ± 4.28[*]
Short tail	0.3 ± 0.82	0.3 ± 0.52	0.5 ± 0.84	0.7 ± 1.21	0.3 ± 0.82
No tail	0.8 ± 1.60	1.5 ± 0.84	1.5 ± 2.35	3.0 ± 1.55	3.5 ± 2.43

[a] Values are presented as means ± SD. [*] $p < 0.05$ vs. NC group; [**] $p < 0.01$ vs. NC group, respectively

group. Compared with the CP group, the MDA content in the CP + CD40 group increased, with no significant difference detected between groups.

Effects of CD on apoptosis

The TUNEL assay was used to investigate testicular apoptotic changes in mice (Fig. 3). Apoptotic cells were scarcely detected in the NC and CD40 groups. However, apoptotic cells were remarkably increased in the CP group when compared with that in the NC group. In addition, the CP + CD40 group exhibited a significantly increased number of apoptotic cells when compared with that in the CP group. The number of apoptotic cells was also higher in the CP + CD20 group than in the CP group; however, no significant differences were detected between the CP and CP + CD20 groups.

Discussion

CD is a type of fine PM that is generated in the Mongolian desert and northern China, and it is of great concern to the health of people living in Northeast Asia including Korea and Japan [11]. According to the previous studies, PM has been reported to induce oxidative stress damage in various organs and impact underlying diseases and drug-mediated actions [16, 18]. CP is known to cause testicular toxicity by triggering oxidative stress [6, 7]. Therefore, we hypothesized that exposure to CD, a type of fine PM, during CP treatment would aggravate the CP-induced oxidative testicular toxicity. In this study, we examined the potential effect of CD exposure on testicular toxicity caused by CP.

As a result of physicochemical analysis, it was found that the morphology of CD was spherical shape, and the actual size of individual particles was 43.4 ± 17.7 nm. CD consisted of O 51.46%, Si 35.38%, Al 6.27%, Fe 5.64%, Mg 0.49%, Ti 0.46%, Ca 0.3%. It has been reported that silica

Table 3 The incidence and severity of histopathological lesions in testes of male mice treated with cyclophosphamide (CP) and/or China dust (CD)

Findings	Grade	Group NC	CP	CD 40	CP + CD 20	CP + CD 40
Testis						
Exfoliation of spermatogenic cells	-	6	3	6	0	0
	+	0	3	0	5	1
	++	0	0	0	1	5
Degeneration of spermatogonia	-	6	0	6	0	0
	+	0	4	0	0	0
	++	0	2	0	6	4
	+++	0	0	0	0	2
Decrease of spermatogonia	-	6	0	6	0	0
	+	0	4	0	0	0
	++	0	2	0	6	3
	+++	0	0	0	0	3
Degeneration of spermatocytes	-	6	0	6	0	0
	+	0	4	0	0	0
	++	0	2	0	6	4
	+++	0	0	0	0	2
Decrease of spermatocytes	-	6	0	6	0	0
	+	0	4	0	0	0
	++	0	2	0	6	4
	+++	0	0	0	0	2
Vacuolation of Sertoli cells	-	6	2	6	0	0
	+	0	4	0	4	0
	++	0	0	0	2	2
	+++	0	0	0	0	4

Grades are as follows: -, normal; +, slight; ++, moderate; and +++, severe change

Fig. 2 Representative photographs of testis sections treated with cyclophosphamide (CP) and/or China dust (CD). Degeneration of spermatocyte/spermatogonia (white arrow), vacuolization (black arrow). Bar = 50 μm
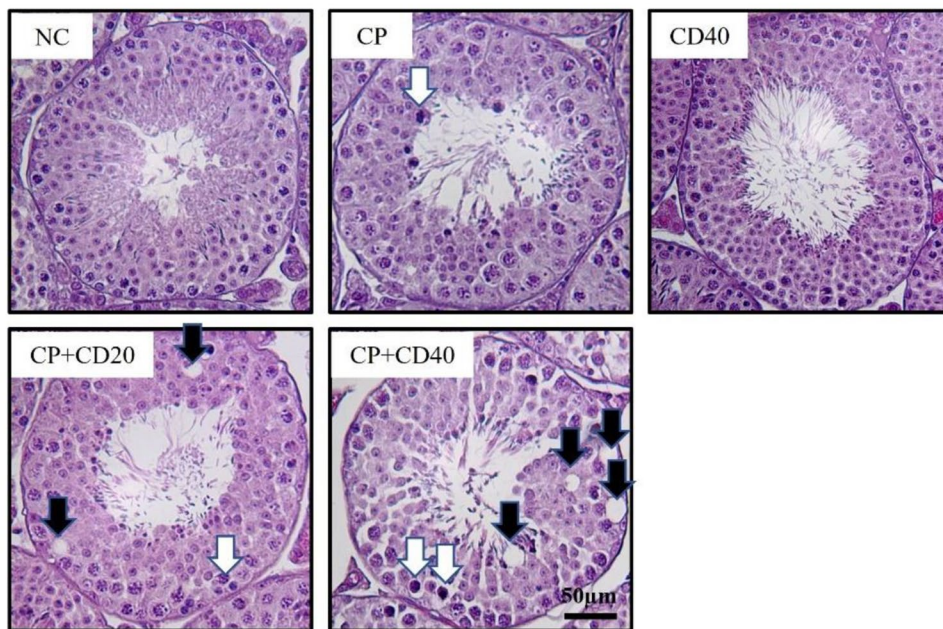
oxide nanoparticles are major component in the Asian sand dust that affects northeast Asian countries, including China, Japan and Korea, especially in the spring, and are associated with the occurrence of various pulmonary diseases across this region [29, 30]. The X-ray spectroscopy analysis confirmed that the major components of CD were silica and oxygen.

Table 4 The number of spermatogenic cells in seminiferous tubules of male mice treated with cyclophosphamide (CP) and/or China dust (CD)

Items		Group				
		NC	CP	CD40	CP + CD20	CP + CD40
Stage II	Spermatogonia	20.6 ± 2.88^a	$7.2 \pm 1.92^{**}$	16.4 ± 3.44	$4.4 \pm 1.34^{**,\dagger}$	$3.8 \pm 1.48^{**,\dagger}$
	Pachytene spermatocytes	51.0 ± 9.14	$29.6 \pm 8.11^{**}$	44.6 ± 5.86	$18.8 \pm 4.09^{**,\dagger}$	$16.0 \pm 3.67^{**,\dagger\dagger}$
	Round spermatids	134.0 ± 21.90	125.8 ± 9.55	122.4 ± 12.30	112.8 ± 9.86	$106.0 \pm 15.79^{*}$
	Elongated spermatids	180.0 ± 13.98	164.8 ± 22.53	165.8 ± 16.86	152.0 ± 31.99	157.0 ± 32.19
	Sertoli cells	12.8 ± 1.92	11.8 ± 2.49	12.2 ± 2.28	12.2 ± 1.79	11.4 ± 2.07
Stage V	Spermatogonia	34.2 ± 4.44	$8.2 \pm 4.21^{**}$	28.6 ± 4.51	$6.0 \pm 4.00^{**}$	$5.8 \pm 3.27^{**}$
	Pachytene spermatocytes	60.0 ± 7.11	$34.4 \pm 9.13^{**}$	48.2 ± 3.77	$21.2 \pm 8.93^{**}$	$17.2 \pm 5.72^{**,\dagger}$
	Round spermatids	153.8 ± 20.78	$106.6 \pm 11.89^{**}$	123.4 ± 11.72	$102.0 \pm 9.92^{**}$	$100.0 \pm 7.07^{**}$
	Elongated spermatids	205.8 ± 21.70	173.4 ± 23.75	202.6 ± 20.92	$158.2 \pm 35.39^{*}$	159.0 ± 40.08
	Sertoli cells	13.6 ± 3.21	11.6 ± 1.14	13.0 ± 2.83	13.0 ± 1.58	11.2 ± 0.84
Stage VII	Spermatogonia	2.0 ± 0.71	2.0 ± 0.71	2.0 ± 0.71	1.6 ± 0.89	2.2 ± 0.84
	Preleptotene spermatocytes	45.8 ± 7.50	$7.8 \pm 1.92^{**}$	37.6 ± 2.97	$3.4 \pm 2.19^{**,\dagger}$	$2.6 \pm 1.82^{**,\dagger\dagger}$
	Pachytene spermatocytes	55.0 ± 9.57	$28.0 \pm 14.63^{**}$	42.8 ± 5.85	29.0 ± 8.00	22.0 ± 7.35
	Round spermatids	155.4 ± 27.75	123.8 ± 14.20	132.2 ± 19.24	$120.8 \pm 28.49^{*}$	$112.8 \pm 6.30^{*}$
	Elongated spermatids	231.0 ± 36.80	202.4 ± 12.90	218.8 ± 18.38	189.0 ± 34.58	181.0 ± 35.94
	Sertoli cells	13.6 ± 1.34	13.2 ± 2.78	12.2 ± 1.92	12.4 ± 1.95	12.2 ± 1.92
Stage XII	Spermatogonia	2.2 ± 0.84	1.8 ± 0.84	2.0 ± 0.71	2.2 ± 0.84	1.8 ± 0.84
	Zygotene spermatocytes	50.8 ± 4.55	$11.6 \pm 2.88^{**}$	46.8 ± 5.26	$6.4 \pm 1.52^{**,\dagger\dagger}$	$4.4 \pm 2.19^{**,\dagger\dagger}$
	Pachytene spermatocytes	65.2 ± 6.22	$37.8 \pm 13.05^{**}$	54.6 ± 5.18	$43.8 \pm 11.08^{**}$	$32.0 \pm 11.05^{**}$
	Elongated spermatids	112.8 ± 13.37	101.0 ± 6.89	115.6 ± 6.80	103.4 ± 9.99	$91.6 \pm 7.13^{**}$
	Sertoli cells	11.4 ± 1.52	12.2 ± 1.30	12.0 ± 2.00	11.8 ± 1.92	12.2 ± 2.77

[a] Values are presented as means $\pm$ SD. $^{*}p < 0.05$ vs. NC group; $^{**}p < 0.01$ vs. NC group; $^{\dagger}p < 0.05$ vs. CP group; $^{\dagger\dagger}p < 0.01$ vs. CP group, respectively

Table 5 Oxidative stress analysis of testis from male mice treated with cyclophosphamide (CP) and/or China dust (CD)

Parameters	Group				
	NC	CP	CD40	CP + CD20	CP + CD40
Glutathione (µmol/mg protein)	191.00 ± 31.32^a	$141.24 \pm 14.76^{**}$	180.63 ± 33.21	$122.59 \pm 19.52^{**}$	$114.30 \pm 13.73^{**,\dagger}$
Glutathione reductase (nmol/min/ml)	519.57 ± 38.63	$453.35 \pm 21.31^{**}$	509.38 ± 50.94	$402.41 \pm 48.99^{**}$	$376.94 \pm 52.20^{**,\dagger}$
Catalase (nmol/min/ml)	166.33 ± 19.83	143.64 ± 32.10	177.59 ± 25.30	$133.79 \pm 18.96^{*}$	$100.14 \pm 25.02^{**,\dagger}$
Malondialdehyde (µmol/mg protein)	31.42 ± 5.67	$37.33 \pm 3.56^{**}$	32.83 ± 3.37	$40.83 \pm 3.87^{**}$	$42.33 \pm 3.44^{**}$

[a] Values are presented as means $\pm$ SD. $^{*}p < 0.05$ vs. NC group; $^{**}p < 0.01$ vs. NC group; $^{\dagger}p < 0.05$ vs. CP group, respectively

In the CP group, the increased occurrence of abnormal clinical manifestation and the significant decline in terminal body weight could be attributed to CP treatment. These results are explicit indicators of systemic toxicity caused by CP administration, correspond with the consequences of former studies [31, 32]. In addition, the occurrence and severity of clinical findings were slightly higher in the CP+CD groups than those observed in the CP group, and the terminal body weight of the CP+CD40 group was significantly decreased compared to that of the CP group. Thus, these findings demonstrated that CD exposure exacerbates the systemic toxicity induced by CP in mice. Furthermore, the absolute weights of the testes and epididymides were affected in the CP group, suggesting that this change in organ weight could directly reflect the overall weight loss.

However, CD exposure in mice had no apparent effect on CP-induced reproductive organ toxicity.

The CP group exhibited decreased sperm motility and increased unusual sperm morphology. The CP+CD groups showed a tendency toward decreased sperm motility; however, this decrease showed no statistical significance when compared to the CP group. Likewise, no remarkable difference in sperm morphology was observed in comparison with the CP group. Therefore, CD exposure failed to demonstrate a clear impact on CP-induced decreased sperm motility and increased abnormal sperm morphology in mice.

Characteristic histopathological findings in the CP group involved exfoliation of spermatogenic cells, degeneration of spermatogonia/spermatocytes, reduced number of spermatogonia/spermatocytes, and vacuolation of Sertoli cells.

Fig. 3 a Representative photographs of TUNEL assay performed on sections of testes treated with cyclophosphamide (CP) and/or China dust (CD). TUNEL positive cells (white arrow). Bar = 100μm. **b** The number of TUNEL-positive cells was counted in five different fields in each section under × 200 magnification. Values are presented as means ± SD. **$p <$ 0.01 vs. NC group; ††$p <$ 0.01 vs. CP group, respectively
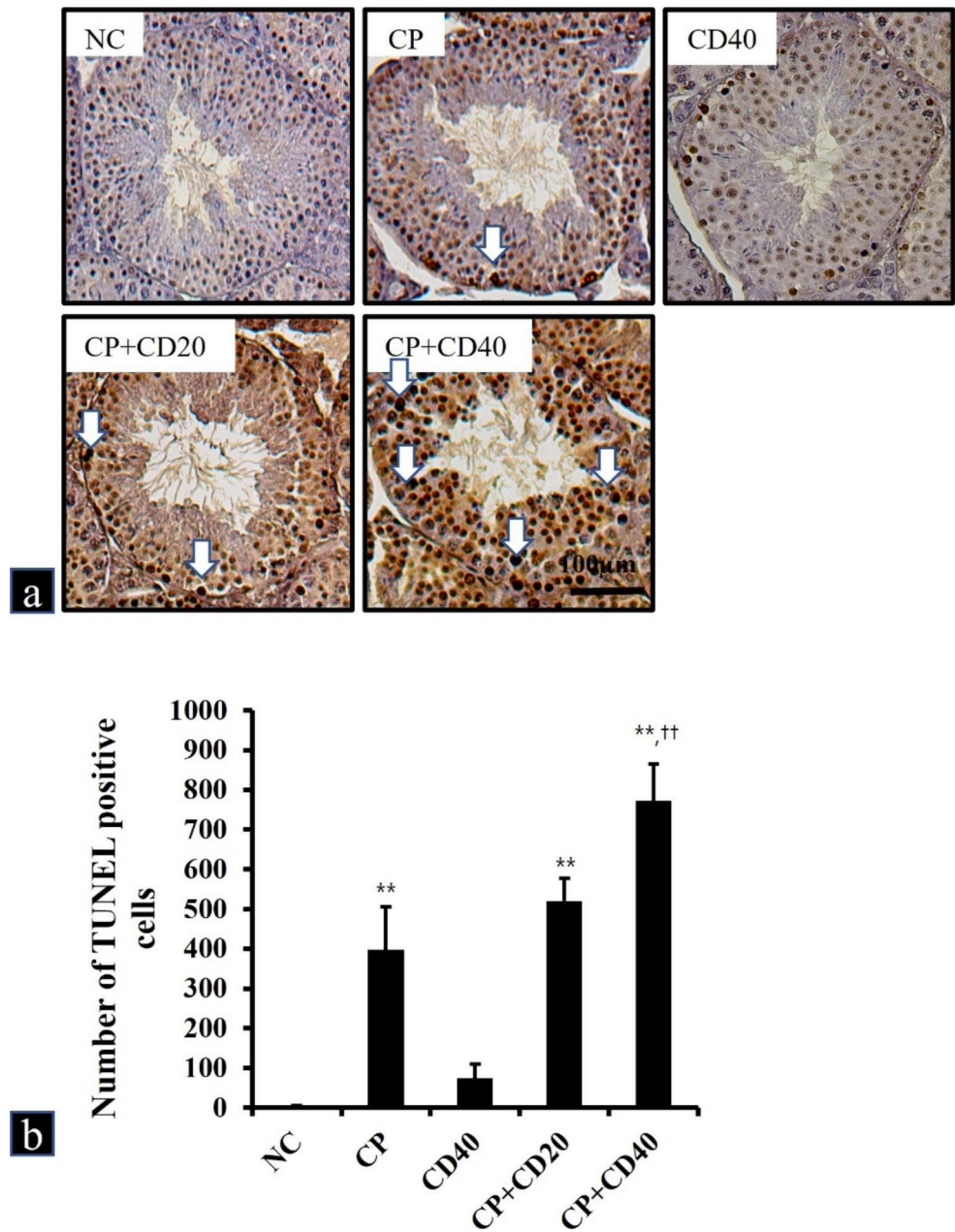
Notably, CP significantly reduced the number of early spermatogenic cells, consistent with previous studies, showing that early spermatogenic cells are the primary target of CP owing to their high mitotic activity [9, 33]. These studies and our histopathological findings demonstrate that CP-induced testicular toxicity may be primarily concentrated on nascent spermatogenic cells undergoing prompt proliferation and differentiation. Further, the occurrence of testicular lesions and the reduced number of nascent spermatogenic cells were more pronounced in the CP + CD groups than in the CP group. Yoshida et al. have reported that intratracheal instillation of natural sand dust in male mice increased the incidence of testicular morphological alterations and

decreased daily sperm production, suggesting male reproductive dysfunction [34]. Additionally, Asian sand dust exposure can affect both fetal development and the reproduction of male offspring in mice [35]. More recently, exposure to $PM_{2.5}$ from automobile exhaust was shown to disrupt spermatogenesis through oxidative stress injury [36]. These findings and our histopathological results suggest that CD exposure may aggravate testicular histological alterations induced by CP.

Mammalian spermatozoa are rich in polyunsaturated fatty acids and inherent deficiency of the intracellular antioxidant enzymes in the testis may also play a role in the susceptibility of spermatozoa to damage by free radicals

[37, 38]. Lipid peroxidation (LPO) by excessive production of semen ROS causes the disintegration of the mitochondrial membrane ultrastructure, which in turn impairs energy metabolism, and reduces sperm motility and viability. It has been reported that oxidative stress caused by LPO is a major cause of CP-induced toxicity and is reportedly mediated by acrolein, a CP metabolite [39]. In the present study, CP treatment decreased GSH content and GR activity and increased MDA content, indicating reduced enzymatic and non-enzymatic antioxidant activities and enhanced LPO. The decrease in GSH content and inhibition of GR and CAT activities were considerably more severe in the CP+CD groups than in the CP group. The increasing MDA concentration observed in the CP+CD groups could be attributed to the elevated CP-induced LPO following CD treatment. Accumulated evidence indicates that PM exposure induces oxidative stress in major organs, leading to inflammation and specific target organ or systemic toxicity [40–42]. These results and our investigation notably demonstrate that an increase in LPO and a decrease in antioxidant activity may be major contributing factors related to CP toxicity, and CD exposure may exacerbate oxidative stress caused by CP.

Apoptosis is a process that keeps homeostasis and is manifested by diverse stimuli, containing ROS-induced oxidative stress [43]. Excessive apoptosis induced by oxidative damage can inhibit spermatogenesis and sperm maturation [44, 45]. It is well-known that CP chemotherapy can induce stage-specific apoptosis in early spermatogenic cells of mice [46, 47]. In this study, CP induced apoptosis in early types of spermatogenic cell, evidenced by TUNEL positive cell count. In addition, CD co-administration remarkably augmented CP-induced apoptotic cells. The findings of apoptosis analysis performed in the CP+CD groups were well correlated with increased testicular toxicity and oxidative stress. This observation is consistent with previous reports indicating that PM exposure induces apoptosis due to ROS-mediated oxidative stress, resulting in testicular toxicity [40, 41]. Although the direct migration of CD to the testis has not been investigated in our experiments, and the precise mechanism of action remains unknown, it has been recently reported that $PM_{2.5}$ contributes to reproductive toxicity by inducing oxidative stress, inflammation, apoptosis, and disruption of the barrier structure of the reproductive system through destroying blood-testis barrier integrity [42]. These previous studies and our present results suggest that CD exposure could increase apoptosis via oxidative damage, thereby exacerbating the testicular toxicity of CP.

In conclusion, CD exposure can exacerbate testicular toxicity induced by CP treatment, which is associated with elevated oxidative stress. Thus, our results provide toxicological evidence that CD exposure can exacerbate CP-induced testicular toxicity, suggesting that CD exposure might aggravate underlying reproductive diseases.

Declarations

Competing interests The authors have no relevant financial or non-financial interests to disclose.

Ethics approval The experimental protocol was performed in accordance with the protocol of the CNU Institutional Animal care and Use Committee (CNU IACUC-YB-2020-109).

Consent to participate Informed consent was obtained from all individual participants included in the study.

References

1. Ahlmann M, Hempel G (2016) The effect of cyclophosphamide on the immune system: implications for clinical cancer therapy. Cancer Chemother Pharmacol 78:661–671. https://doi.org/10.1007/s00280-016-3152-1

2. Emadi A, Jones RJ, Brodsky RA (2009) Cyclophosphamide and cancer: golden anniversary. Nat Rev Clin Oncol 6:638–647. https://doi.org/10.1038/nrclinonc.2009.146

3. Ghobadi E, Moloudizargari M, Asghari MH, Abdollahi M (2017) The mechanisms of cyclophosphamide-induced testicular toxicity and the protective agents. Expert Opin Drug Metab Toxicol 13:525–536. https://doi.org/10.1080/17425255.2017.1277205

4. Das UB, Mallick M, Debnath JM, Ghosh D (2002) Protective effect of ascorbic acid on cyclophosphamide-induced testicular gametogenic and androgenic disorders in male rats. Asian J Androl 4:201–207. https://pubmed.ncbi.nlm.nih.gov/12364977/

5. Hoorweg-Nijman JJ, Delemarre-van de Waal HA, de Waal FC, Behrendt H (1992) Cyclophosphamide-induced disturbance of gonadotropin secretion manifesting testicular damage. Acta Endocrinol (Copenh) 126:143–148. https://doi.org/10.1530/acta.0.1260143

6. Ghosh D, Das UB, Ghosh S, Mallick M (2002) Testicular gametogenic and steroidogenic activities in cyclophosphamide treated

rat: a correlative study with testicular oxidative stress. Drug Chem Toxicol 25:281–292. https://doi.org/10.1081/dct-120005891

7. Liu F, Li XL, Lin T, He DW, Wei GH et al (2012) The cyclophosphamide metabolite, acrolein, induces cytoskeletal changes and oxidative stress in Sertoli cells. Mol Biol Rep 39:493–500. https://doi.org/10.1007/s11033-011-0763-9

8. Haenen GR, Vermeulen NP, Tai-Tin-Tsoi JN, Ragetli HM, Timmerman H et al (1988) Activation of the microsomal glutathione-S-transferase and reduction of the glutathione dependent protection against lipid peroxidation by acrolein. Biochem Pharmacol 37:1933–1938. https://doi.org/10.1016/0006-2952(88)90539-4

9. Kim SH, Lee IC, Ko JW, Shin IS, Moon C et al (2016) Mechanism of protection by diallyl disulfide against cyclophosphamide-induced spermatotoxicity and oxidative stress in rats. Mol Cell Toxicol 12:301–312. https://doi.org/10.1007/s13273-016-0035-9

10. Ertmer F, Oldenhof H, Schütze S, Rohn K, Wolkers WF et al (2017) Induced sub-lethal oxidative damage affects osmotic tolerance and cryosurvival of spermatozoa. Reprod Fertil 29:1739–1750. https://doi.org/10.1071/RD16183

11. Kim K, Kim SD, Shin TH, Bae CS, Ahn T et al (2021) Respiratory and systemic toxicity of inhaled artificial Asian sand dust in pigs. Life (Basel) 11:25. https://doi.org/10.3390/life11010025

12. Hashizume M, Kim Y, Ng CFS, Chung Y, Madaniyazi L et al (2020) Health effects of Asian dust: a systematic review and meta-analysis. Environ Health Perspect 128:66001. https://doi.org/10.1289/EHP5312

13. Cheung K, Daher N, Kam W, Shafer MM, Ning Z et al (2011) Spatial and temporal variation of chemical composition and mass closure of ambient coarse particulate matter ($PM_{10-2.5}$) in the Los Angeles area. Atmos Environ 45:2651–2662. https://doi.org/10.1016/j.atmosenv.2011.02.066

14. Mori I, Nishikawa M, Tanimura T, Quan H (2003) Change in size distribution and chemical composition of kosa (Asian dust) aerosol during long-range transport. Atmos Environ 37:4253–4263. https://doi.org/10.1016/S1352-2310(03)00535-1

15. Gualtieri M, Ovrevik J, Mollerup S, Asare N, Longhin E et al (2011) Airborne urban particles (Milan winter-$PM_{2.5}$) cause mitotic arrest and cell death: effects on DNA, mitochondria, AhR binding and spindle organization. Mutat Res 713:18–31. https://doi.org/10.1016/j.mrfmmm.2011.05.011

16. Øvrevik J (2019) Oxidative potential versus biological effects: a review on the relevance of cell-free/abiotic assays as predictors of toxicity from airborne particulate matter. Int J Mol Sci 20:4772. https://doi.org/10.3390/ijms20194772

17. Li N, Xia T, Nel AE (2008) The role of oxidative stress in ambient particulate matter-induced lung diseases and its implications in the toxicity of engineered nanoparticles. Free Radic Biol Med 44:1689–1699. https://doi.org/10.1016/j.freeradbiomed.2008.01.028

18. Møller P, Danielsen PH, Karottki DG, Jantzen K, Roursgaard M et al (2014) Oxidative stress and inflammation generated DNA damage by exposure to air pollution particles. Mutat Res Rev Mutat Res 762:133–166. https://doi.org/10.1016/j.mrrev.2014.09.001

19. NRC (National Research Council) (2011) Guide for the Care and Use of Laboratory Animals. National Research Council, National Academy, Washington, USA

20. Lee KH, Lee DW, Kang BC (2020) The 'R' principles in laboratory animal experiments. Lab Anim Res 36:45. https://doi.org/10.1186/s42826-020-00078-6

21. Abd-El-Tawab AM, Shahin NN, AbdelMohsen MM (2014) Protective effect of Satureja montana extract on cyclophosphamide-induced testicular injury in rats. Chem Biol Interact 224:196–205. https://doi.org/10.1016/j.cbi.2014.11.001

22. Chabra A, Shokrzadeh M, Naghshvar F, Salehi F, Ahmadi A (2014) Melatonin ameliorates oxidative stress and reproductive

toxicity induced by cyclophosphamide in male mice. Hum Exp Toxicol 33:185–195. https://doi.org/10.1177/0960327113489052

23. Ko JW, Shin NR, Je-Oh L, Jung TY, Moon C et al (2020) Silica dioxide nanoparticles aggravate airway inflammation in an asthmatic mouse model via NLRP3 inflammasome activation. Regul Toxicol Pharmacol 112:104618. https://doi.org/10.1016/j.yrtph.2020.104618

24. Park EJ, Kang MS, Jin SW, Lee TG, Lee GH et al (2021) Multiple pathways of alveolar macrophage death contribute to pulmonary inflammation induced by silica nanoparticles. Nanotoxicology 15:1087–1101. https://doi.org/10.1080/17435390.2021.1969461

25. Lee KM, Lee IC, Kim SH, Moon C, Park SH et al (2012) Melatonin attenuates doxorubicin-induced testicular toxicity in rats. Andrologia 44:796–803. https://doi.org/10.1111/j.1439-0272.2011.01269.x

26. Beladiya JV, Mehta AA (2021) Acute and 28-days subacute toxicity studies of Gαq-RGS2 signaling inhibitor. Lab Anim Res 37:17. https://doi.org/10.1186/s42826-021-00093-1

27. Jeong YJ, Jeon H, Kim EJ, Ryu HY, Song KS et al (2022) Evaluation of the acute, sub-chronic and chronic oral toxicity, genetic toxicity, and safety of a Lomens-Po. Toxicol Res 38:69–90. https://doi.org/10.1007/s43188-021-00090-5

28. Oakberg EF (1956) A description of spermiogenesis in the mouse and its use in analysis of the cycle of the seminiferous epithelium and germ cell renewal. Am J Anat 99:391–413. https://doi.org/10.1002/aja.1000990303

29. Yang HW, Park JH, Shin JM, Lee HM, Park IH (2019) Asian sand dust upregulates IL-6 and IL-8 via ROS, JNK, ERK, and CREB signaling in human nasal fibroblasts. Am J Rhinol Allergy 34:249–261. https://doi.org/10.1177/1945892419890267

30. Lim JO, Lee SJ, Kim WI, Pak SW, Kim JC et al (2021) Melatonin alleviates silica nanoparticle-induced lung inflammation via thioredoxin-interacting protein downregulation. Antioxidants 10:1765. https://doi.org/10.3390/antiox10111765

31. Kim SH, Lee IC, Baek HS, Moon C, Kim SH et al (2013) Protective effect of diallyl disulfide on cyclophosphamide-induced testicular toxicity in rats. Lab Anim Res 29:204–211. https://doi.org/10.5625/lar.2013.29.4.204

32. Tripathi DN, Jena GB (2008) Astaxanthin inhibits cytotoxic and genotoxic effects of cyclophosphamide in mice germ cells. Toxicology 248:96–103. https://doi.org/10.1016/j.tox.2008.03.015

33. Ilbey YO, Ozbek E, Simsek A, Otunctemur A, Cekmen M et al (2009) Potential chemoprotective effect of melatonin in cyclophosphamide- and cisplatin-induced testicular damage in rats. Fertil Steril 92:1124–1132. https://doi.org/10.1016/j.fertnstert.2008.07.1758

34. Yoshida S, Hiyoshi K, Ichinose T, Nishikawa M, Takano H et al (2009) Aggravating effect of natural sand dust on male reproductive function in mice. Reprod Med Biol 8:151–156. https://doi.org/10.1007/s12522-009-0027-8

35. Yoshida S, Ichinose T, Arashidani K, He M, Takano H et al (2016) Effects of fetal exposure to Asian sand dust on development and reproduction in male offspring. Int J Environ Res Public Health 13:1173. https://doi.org/10.3390/ijerph13111173

36. Liu B, Wu SD, Shen LJ, Zhao TX, Wei Y et al (2019) Spermatogenesis dysfunction induced by $PM_{2.5}$ from automobile exhaust via the ROS-mediated MAPK signaling pathway. Ecotoxicol Environ Saf 167:161–168. https://doi.org/10.1016/j.ecoenv.2018.09.118

37. Sikka SC (2004) Role of oxidative stress and antioxidants in andrology and assisted reproductive technology. J Androl 25:5–18. https://doi.org/10.1002/j.1939-4640.2004.tb02751.x

38. Palani AF (2018) Effect of serum antioxidant levels on sperm function in infertile male. Mid East Fertil Soc J 23:19–22. https://doi.org/10.1016/j.mefs.2017.07.006

39. Motawi TM, Sadik NA, Refaat A (2010) Cytoprotective effects of DL-alpha-lipoic acid or squalene on cyclophosphamide-induced oxidative injury: an experimental study on rat myocardium, testicles and urinary bladder. Food Chem Toxicol 48:2326–2336. https://doi.org/10.1016/j.fct.2010.05.067

40. Liu J, Zhang J, Ren L, Wei J, Zhu Y et al (2019) Fine particulate matters induce apoptosis via the ATM/P53/CDK2 and mitochondria apoptosis pathway triggered by oxidative stress in rat and GC-2spd cell. Ecotoxicol Environ Saf 180:280–287. https://doi.org/10.1016/j.ecoenv.2019.05.013

41. Wei Y, Cao XN, Tang XL, Shen LJ, Lin T et al (2018) Urban fine particulate matter (PM$_{2.5}$) exposure destroys blood-testis barrier (BTB) integrity through excessive ROS-mediated autophagy. Toxicol Mech Methods 28:302–319. https://doi.org/10.1080/15376516.2017.1410743

42. Wang L, Luo D, Liu X, Zhu J, Wang F et al (2021) Effects of PM$_{2.5}$ exposure on reproductive system and its mechanisms. Chemosphere 264:128436. https://doi.org/10.1016/j.chemosphere.2020.128436

43. Kaczanowski S (2016) Apoptosis: its origin, history, maintenance and the medical implications for cancer and aging. Phys Biol 13:031001. https://doi.org/10.1088/1478-3975/13/3/031001

44. Guo H, Ouyang Y, Wang J, Cui H, Deng H et al (2021) Cu-induced spermatogenesis disease is related to oxidative stress-mediated germ cell apoptosis and DNA damage. J Hazard Mater 416:125903. https://doi.org/10.1016/j.jhazmat.2021.125903

45. Shukla KK, Mahdi AA, Rajender S (2012) Apoptosis, spermatogenesis and male infertility. Front Biosci (Elite Ed) 4:746–754. https://doi.org/10.2741/415

46. Boekelheide K (2005) Mechanisms of toxic damage to spermatogenesis. J Natl Cancer Inst Monogr 34:6–8. https://doi.org/10.1093/jncimonographs/lgi006

47. Cai L, Hales BF, Robaire B (1997) Induction of apoptosis in the germ cells of adult male rats after exposure to cyclophosphamide. Biol Reprod 56:1490–1497. https://doi.org/10.1095/biolreprod56.6.1490